Factors behind intraspecific competition during post-glacial recolonization: a Norway spruce case study

Tiret M.[1,2*], Olsson L.[3], Grahn T.[3], Karlsson B.[4], Milesi P.[1], Lascoux M.[1], Lundqvist S.-O.[3,5], García-Gil M.R.[2]

[1] Program in Plant Ecology and Evolution, Department of Ecology and Genetics, EBC and SciLife Lab, Uppsala University, Sweden.

[2] Department of Forest Genetics and Plant Physiology, SLU, Umeå Plant Science Centre (UPSC), Umeå, Sweden.

[3] RISE Bioeconomy, Box 5604, 114 86 Stockholm, Sweden.

[4] Skogforsk, Ekebo, 2250 SE-268 90 Svalöv, Sweden.

[5] IIC, Rosenlundsgatan 48B, 11863 Stockholm, Sweden.

*: corresponding author: Mathieu Tiret, **Email**: mathieu.tiret@ebc.uu.se

Summary:

- To a large extent, the current distribution and population structure of many species were shaped by the cycles of isolation in glacial refugia and subsequent population expansions. Isolation in, and post-glacial expansion through, heterogeneous environments led to either neutral or adaptive divergence. Norway spruce is no exception, and its current distribution is the consequence of a complex interplay between evolutionary forces.
- We investigated population differentiation and adaptations of Norway spruce for juvenile growth, diameter of the trunk at breast height and its components: wood density and tracheid traits. Data from 4,461 phenotyped and genotyped Norway spruce from 396 half-sib families in two progeny tests were used to test for divergent selection in the framework of Q_{ST} vs F_{ST}, and to carry out multiple Genome-Wide Association Studies.
- We show that (i) the macroscopic resultant trait (trunk diameter), unlike its microscopic components (tracheid dimensions) and juvenile growth, was under divergent selection, and (ii) adaptation predated the Last Glaciation Maximum.
- Altogether, the current variation in these phenotypic traits in Norway spruce is better explained by local adaptation to ancestral environments than to current ones, where populations were partly pre-adapted mainly through growth-related traits.

199 words / 200 max.

main text: 6285 words / 6500 max.
5 figures.
1 table.

Keywords: Norway spruce, wood quality, population structure, competition, GWAS, Q_{ST}.

Introduction

During the Quaternary glacial cycles, many European animal and plant species were confined to southern refugia. Those were often located in the Iberian, Italian and the Balkan peninsulas, but surviving populations could also be distributed on less discrete spots and, instead, scattered along the southern edge of the ice sheet (Bennett, 1997; Binney et al., 2009; Kremer et al., 2010). Improvement of climatic conditions during the post-glacial periods led to demographic expansions accompanied by population admixture (e.g., Petit et al., 2003), new selective pressures (e.g., Suarez & Tsuitsui, 2008), and inter and/or intraspecific competition (e.g., Savolainen et al., 2007). Although the present population structure is the result of successive cycles of glaciation events that led to a series of demographic contractions and expansions, the current distribution of many species has, at least in part, been shaped by the different selective pressures that acted during the period after the Last Glacial Maximum (e.g., Petit et al., 2002; Palmé et al., 2003).

During this period, new abiotic and biotic pressures presumably led to new adaptations. Selection acts upon relative fitness and thereby primarily depends on the biotic environment (Red Queen hypothesis, Van Valen, 1973): in a sense, selection *is* competition. In many tree species, current phenotypes reflect past selection and competition (Von Gadow et al., 2021), and competition is known to play an important role in shaping species distribution (Case et al., 2005; Savolainen et al., 2007; Wisz et al., 2013). In the particular case of competition for light and space, wood is an important tissue, since radial growth of the woody stem provides the mechanical support for woody plants to grow tall and gain a competitive advantage (Givnish, 1982; Iwasa, 1985; Falster & Westoby, 2003; Falster & Westoby, 2005). However, adaptation for upright growth, increasing competitiveness, is often associated with modified wood properties and evolutionary trade-offs (Poorter et al., 2006; Chave et al., 2009). Wood density is a good example of such a growth-survival trade-off (Kitajima 1994; Poorter et al., 2010), where low wood density, resulting from wider lumina and, in hardwood species, wider vessels (e.g., Enquist et al., 1999; Preston et al., 2006; Coomes et al., 2008), is associated with fast growth. Conversely, high wood density provides higher biomechanical safety (e.g., Niklas, 1993; Van Gelder et al., 2006) and resistance against pathogens (Augspurger & Kelly, 1984), and is thus associated with higher survival rates. The growth-survival trade-off is a common ecological trade-off observed in both tropical (e.g., Faster & Westoby, 2005; Poorter, 2008) and boreal species (e.g., Rossi et al., 2015; Pretzsch et al., 2018).

Norway spruce (*Picea abies* (L.) H. Karst.) is a dominant boreal conifer species that thrives nowadays in a vast northern domain spanning from Norway to central Russia, as well as in two smaller domains in the Alps and the Carpathians (Vendramin et al., 2000; Tsuda et al., 2016; Nota et al., 2022). Repeated demographic movements associated to climatic cycles and ensuing secondary contacts led to the division of Norway spruce into seven genetic clusters (Chen et al., 2019): Central and South Sweden (CSE), Russia-Baltics (RBA), Northern Poland (NPL), Central Europe (CEU), Alps (ALP), Carpathians (ROM), and hybrids between CSE and ALP (CSE-ALP). In the present paper, to obtain a comprehensive picture of factors behind selection acting during the post-glacial expansion of Norway spruce, and possibly competition, we investigated population differentiation and tested for adaptive signature or trade-offs associated to trunk diameter and wood density. Since the nature of competition between trees is expected to change over ontogenetic stages (Miriti, 2006), we studied the development of these phenotypes with cambial age/ring number, and some related tracheid traits from increment cores sampled from two progeny trials of the Swedish breeding program. We have conducted the analyses on a large dataset of 4,461 twenty-year-old trees from 396 half-sib families, 118,145 SNPs from exome sequencing. We show that (i) the macroscopic resultant trait (diameter of the trunk at breast height), unlike its components (tracheid dimensions), was most likely under divergent selection, and (ii) the structure of the current variation in these phenotypic traits within Norway spruce is better explained by adaptation to ancestral environments than to current ones.

Materials and Methods

Plant material. The study is based on data previously published (Chen et al., 2014; Chen et al., 2016; Lundqvist et al., 2018), which are here analyzed with a special attention to population structure and selection. The data originate from two progeny trials of Norway spruce at two different sites: FF1146 (Höreda, Sweden; 57°60'N 15°04'E), and FF1147 (Erikstorp, Sweden; 56°80'N 13°90'E). Both trials were established by the Forestry Research Institute of Sweden (Skogforsk) in the spring of 1990 from open-pollinated seeds harvested on selected trees from 112 stands in southern Sweden. FF1146 comprised 1,373 half-sib families and FF1147, 1,375 half-sib families. In both trials, a randomized incomplete block design was implemented (20 blocks in FF1146, 23 in FF1147), with single-tree plots and a homogeneous spacing of 1.4 m x 1.4 m. Dead trees and trees of low breeding interest were removed in 2008. After filtering out (i) half-sib families absent in the established Skogforsk clonal archives, and (ii) stands with less than three half-sib families, the study included a total of 518 half-sib families with 5,644 progenies (2,983 from FF1146, and 2,661 from FF1147).

Population structure. Population structure was previously assessed at a fine scale by Chen et al. (2019), using 399,801 unlinked non-coding SNPs on 1,672 individuals, categorizing families into the following genetic clusters (ordered by decreasing latitude): Central and South Sweden (CSE), Russia-Baltics (RBA), Northern Poland (NPL), Central Europe (CEU), Alps (ALP), Carpathians (ROM), and hybrids between CSE and ALP (CSE-ALP) (for tree original locations, see Fig. 1 of Milesi et al., 2019). The families examined in this study followed the same genetic clustering (Fig. 1A, 1B). Individuals from the ROM genetic cluster were removed, as our sample included only three such families, whereas all other clusters included at least ten families (Table S1).

Phenotype measurements. Increment cores of 12 mm diameter, extracted from the northern side of the stem, were collected in 2010 and 2011 at breast height (BH, 1.3 m above the ground) from six trees per half-sib family per trial. Trees were 20 or 21 years old, which is young compared to the usual cutting age of 60-70 years or higher. The increment cores were then analyzed by SilviScan (Evans, 1994, 2006) at Innventia, now RISE (Stockholm, Sweden), assessing high-resolution pith-to-bark radial variation in growth, tracheid and wood properties. In this study, we focused on the development with cambial age (ring number) of ring width (RW, in mm), and ring means for wood density (WD, in kg/m^3), tracheid radial width (TRW, in µm), tracheid tangential width (TTW, in µm), tracheid

wall thickness (TWT, in µm), diameter at breast height (DBH, in mm) calculated from ring widths, and the age when the trees reached breast height (ABH). The measurements, identification of annual rings and the importance of ABH are discussed in Lundqvist et al. (2018).

The two innermost rings were removed as the extremely curved structure of the xylem does not allow the same high data quality as for rings further out. In addition, only data up to the 13th ring was kept for analyses, since only fast-growing offspring with low ABH are represented at the highest cambial ages. To avoid the effect of thinning, we removed all annual rings formed after 2008, involving only slow-grown trees which had not formed a 13th ring at that age. The study then covered six traits (RW, WD, TRW, TTW, TWT, DBH) for 11 rings per offspring in most of the cases, and their ABH.

Exome capture and SNP filtering. The exome capture (target re-sequencing) of the mother of each half-sib family is available on BioProject PRJNA511374 (Chen et al., 2019) and BioProject PRJNA731384 (Chen et al., 2021). Total genomic data was extracted from the buds of the 518 maternal trees (or needles when buds were not available) using the Qiagen Plant DNA extraction kit (Qiagen, Germany). DNA concentration was assessed using the Qubit® ds DNA Broad Range Assay Kit (Oregon, USA). The extracted DNA was sent to RAPiD Genomics (Gainesville, USA) for library preparation and exome sequencing. Sequence capture, with an average depth of 15X, was performed using the Illumina HiSeq 2500 (San Diego, USA), with 40,018 diploid probes (120bp-length) designed to capture 26,219 genes of *P. abies* (Vidalis et al., 2018). After mapping the raw reads against the *P. abies* reference genome v1.0 (Nystedt et al., 2013) using BWA-MEM with default settings (Li & Durbin, 2010), PCR duplicates were sorted and marked using SAMTOOLS v1.2 (Li et al., 2009) and Picard v1.141 (http://broadinstitute.github.io/picard). INDELs were realigned using GATK v3.5.0 (McKenna et al., 2010). Variant calling was performed using GATK HaplotypeCaller v3.6, non-biallelic SNPs were filtered out using GATK SelectVariants v3.6 (option --restrict-alleles-to BIALLELIC), and quality filtering was carried out by the Variant Quality Score Recalibration following the procedure of Van der Auwera et al. (2013).

As an alternative way to account for Minor Allele Frequency (MAF), we filtered out SNPs with less than five individuals per genotype to avoid a leverage effect biasing GWASs. We performed a loose filtering for variant call rate (or missingness) with PLINK v1.9 (Chang et al., 2015), by removing individuals with more than 70% SNP-missingness, resulting in 472

half-sib families, and by removing SNPs with more than 70% individual-missingness, resulting in 118,145 SNPs (each mother is then genotyped for at least 35,443 SNPs). 70,277 SNPs were successfully mapped on the consensus map of Bernhardsson et al. (2019).

Statistical model. The traits (DBH, WD, RW, TRW, TTW, and TWT) were normalized by their respective overall means (across all trees and rings 3 to 13) to allow comparison between traits. Then, they were analyzed at each cambial age separately, resulting in six traits over 11 rings, so a total of 66 traits in addition to ABH.

To study the family effect underlying the traits, we used the following mixed model:

$$Y_{ijkl} = \mu + s_i + B_{ij} + F_k + \varepsilon_{ijkl}, \qquad (1)$$

where 'Y_{ijkl}' is the trait of the l-th offspring of the k-th family in the j-th block at the i-th site, 'μ' is the grand mean, 's_i' is the fixed effect of the i-th site, 'B_{ij}' and 'F_k' are uncorrelated random effects of the j-th block nested in i-th site (with variance σ_F^2) and the k-th half-sib family (with variance σ_B^2) respectively, and 'ε_{ijkl}' the residual fitted to a Gaussian distribution of variance σ^2. The family effect was not fitted using a kinship matrix, thus potentially overestimating its effect and providing an upper bound. Heritability was estimated as $4 \times \sigma_F^2 / (\sigma_F^2 + \sigma_B^2 + \sigma^2)$ as an intraclass correlation estimation of half-sib families (p.166, Falconer, 1989). In parallel, to study the effect of population structure, we used the following mixed model:

$$Y_{ijkl} = \mu + s_i + g_k + B_{ij} + F_k + \varepsilon_{ijkl}, \qquad (1bis)$$

where 'g_k' is the fixed effect of the k-th family's genetic cluster, and the other terms are as defined above in model (1). The estimated family effects of both model (1) and (1bis) were used as input for subsequent GWASs.

To investigate the effect of genetic clusters on traits jointly with the effect of ABH, we used the following linear mixed model:

$$Y_{ijkl} = \mu + c_l + s_i + g_k + (c \times g)_l + (c \times s)_l + B_{ij} + F_k + \varepsilon_{ijkl}, \qquad (2)$$

where 'c_l' is the fixed effect of the l-th offspring's ABH, '$(c \times g)_l$' is the fixed interaction effect between ABH and the genetic cluster of the l-th offspring, '$(c \times s)_l$' is the fixed interaction effect between ABH and the site of the l-th offspring, and the other terms are as defined

above in models (1) and (1bis). Model (2) was applied on the 66 traits, as previously mentioned.

Finally, to disentangle the effect of divergent selection and neutral divergence, we estimated Q_{ST} as defined by Spitze (1993) with the following mixed model:

$$Y_{ijkl} = \mu + s_i + G_k + B_{ij} + F_k + \varepsilon_{ijkl}, \qquad (3)$$

where 'G_k' is the random effect of the k-th family's genetic cluster (with variance σ_A^2), and the other terms are as defined above in model (1). Q_{ST} was estimated as $\sigma_A^2/(\sigma_A^2 + 2\sigma_B^2)$, and averaged across rings. Following the recommendation of Whitlock (2008), we compared Q_{ST} to the positive part of the distribution of F_{ST} computed on non-coding genes (with VCFTools v0.1.16, option --weir-fst-pop; Danecek et al., 2011). The set of non-coding genes were obtained without filtering for MAF or missingness, amounting then to 789,786 SNPs. If Q_{ST} of a trait is significantly larger than F_{ST}, the trait can be considered to have diversified more than expected under neutrality in a heterogeneous environment. In contrast, if Q_{ST} cannot be distinguished from F_{ST} values, we would have little evidence that selection is responsible for phenotypic divergence.

All computations were done using R v4.0.4 (R core team, 2021), and all models were fitted with the R package *lme4* (function *lmer*; Bates et al., 2015). Statistical significance of the fixed effects was assessed using a type II Wald chi-square test (function *Anova* of the R package *car*), and significance of a slope was assessed using a Student *t*-test. To account for the unbalance caused by consecutive filtering, we only kept families with at least four offspring per site. Applying all the previous filters, we ended up with 396 half-sib families and 4,461 offspring per trait.

Genome-Wide Association Study. GWAS was performed on the estimated family effect of model (1) and model (1bis). We fitted each SNP individually, with or without a population structure correction by including the genetic cluster as a covariate (model (1) or model (1bis) respectively). We also used the software GCTA (option --mlma; Yang et al., 2011) that included a polygenic effect. GWAS not including kinship was referred to (M) when not corrected for population structure, and (M*) when corrected for population structure. GWAS including kinship (from GCTA) was referred to (K) when not corrected for population structure, and (K*) when corrected for population structure. GWAS (K*) would be the classic GWAS. For significant SNPs, we re-estimated the effect size by using an empirical Bayes

approach for adaptive shrinkage with the R package *ashr* (function *ash*; Stephens, 2017). In order to assess the quality of a GWAS through its Q-Q plot, we introduce the distance D as the distance between the highest log p-value (the rightmost value on a Q-Q plot) and the highest upper bound of the 95% confidence interval of a uniform distribution. If the distance D is positive, it means that some SNPs are more significant than expected; if D is between 0 and −2.16 (the width of the confidence interval for n = 118,145), the p-value distribution follows a uniform distribution with a confidence level of 95%; and if D is below −2.16, the SNPs are less significant than expected, suggesting an overcorrection by population structure. Additionally, in order to detect regions with high density of significant SNPs - namely peaks - we used a custom peak detection script with default settings (Tiret & Milesi, 2021), which is freely available at https://github.com/milesilab/peakdetection (see details in Li et al., preprint).

Results

The ontogenetic shifts across the first 20 years have been previously investigated with the same data (Chen et al., 2014, 2016; Lundqvist et al., 2018). Here, the data were analyzed in a more evolutionary perspective.

Overall variation at different ages and among populations

The overall variability of the six traits (DBH, WD, RW, TRW, TTW, and TWT) was rather similar across the cambial ages investigated (Fig. 1C). A comparison of the coefficients of variation (CV) at the different ages for those traits (Fig. S1) showed that DBH was the only trait whose CV significantly decreased with age (Student's t = -6.13, $p < 0.001$). Heritability on the 13th annual ring ranged from 20.87% to 49.80% (Table 1, Fig. 2H), in accordance with previous studies (Hannrup et al., 2004; Chen et al., 2014, 2021).

The six phenotypes also differed among genetic clusters, though to a lesser extent than ontogenetic shift (Fig. 2). DBH was higher, and WD and ABH lower in Southern populations, in accordance with previous reports (Rossi et al., 2015; Montwé et al., 2016; Milesi et al., 2019). In addition to the longer growth period of southern individuals (Chen et al., 2012), every trait of the southern populations was consistent with higher investment in growth than in wood density, which is also translated into higher RW, TRW and TTW and lower TWT (Fig. 2). Individuals from the cluster CSE-ALP were phenotypically closer to ALP than to CSE.

ABH mostly impacts DBH at young ages and is population specific

ABH is determined by both genetics and environment, as both the site effect (χ^2 = 26.6, degree of freedom or df = 5, p = 3.05 x 10^{-5}) and the genetic cluster effect (χ^2 = 102.8, df = 1, p < 10^{-5}) had a highly significant effect on ABH in model (1bis). ABH had a relatively higher environmental variance, which led to a relatively lower heritability of 20.87% compared to other traits (Table 1, Fig. 2H). The lower heritability was not due to a lower genetic variance of ABH, in fact quite the opposite (Table 1). ABH was latitudinally structured, half-sib families of southern origin having a low ABH, i.e., faster early height growth rates (Fig. 2A, 3A). Despite the fact that ABH significantly depends on genetics in model (1bis), its interaction with the genetic cluster effect in model (2) was less determinant than the direct effect of ABH and its interaction with site effect on the 66 traits: at a Bonferroni adjusted cut-off of p = 7.58 x 10^{-3} (66 traits), ABH and its interaction with the site effect were significant for 47 and 30

traits, respectively, while its interaction with the genetic cluster effect was significant for only two traits (Table S2). To account for the significant interaction between ABH and site effect, we split the dataset as recommended by Crawley (2007, pp. 323–386). The subsequent analyses are focusing on the Höreda trial, but the conclusions were the same in the Erikstorp trial.

Apart from ring width, early growth rate mostly impacted early or later ring traits, less so at cambial ages 5-7 (Fig. 3B). For early rings (3rd and 4th rings), ABH significantly impacted every trait but the 4th ring WD (χ^2 = 7.77, df = 1, p = 5.32 x 10^{-3}, in model (2) with a Bonferroni cut-off of p = 7.58 x 10^{-3}). For intermediate rings (5th to 8th rings), ABH significantly impacted only 6 out of 20 traits (χ^2 > 16.4, df = 1, p < 1 x 10^{-5}). For later rings (from the 9th ring), ABH significantly impacted every trait but the 9th ring TTW (χ^2 = 4.05, df = 1, p = 4.41 x 10^{-2}), the 11th ring TWT (χ^2 = 7.09, df = 1, p = 7.76 x 10^{-3}) and the 12th ring TWT (χ^2 = 4.57 x 10^{-3}, df = 1, p = 0.98). For ring width, the results showed that early growth rate mostly impacted intermediate and later rings (5th to 11th rings), as the significance of ABH followed a concave curve starting with an increase from the 5th ring (χ^2 = 31.71, df = 1, p < 10^{-5}) up until the 9th ring (χ^2 = 1045.15, df = 1, p < 10^{-5}), then a decrease until the 13th ring (χ^2 = 40.19, df = 1, p < 10^{-5}). This can also be understood from Fig. 5a of Lundqvist et al. (2018), where similar age curves, shifting sidewise with ABH, have their steepest phase during the intermediate cambial ages.

Trees with a low ABH, i.e., fast growers, ended up on the one hand with a markedly larger DBH (negative effect on the Fig. 3C), though smaller at the beginning, and on the other hand, with lower WD and TWT, and slightly higher TRW and TTW (Fig. 3C, S2). Fast growers had increasingly higher DBH over time, as the effect of ABH decreased from the 3rd ring to the 13th ring (from 1.75 x 10^{-2} ± 0.00684 to – 9.51 x 10^{-2} ± 0.0525). On the opposite, fast growers had increasingly lower WD, as the effect of ABH increased from the 3rd ring to the 13th ring (from 1.10 x 10^{-2} ± 0.00507 to 4.95 x 10^{-2} ± 0.0105). However, fast growers were not distinguishable in terms of tracheid properties (TRW, TTW, TWT), as the effect of ABH remained low from the 3rd ring to the 13th ring (from 1.12 x 10^{-2} ± 0.00682 to 5.39 x 10^{-3} ± 0.0296). Fast growers also had significantly larger 9th rings, as the effect of ABH on RW followed a convex curve matching its concave significance, reaching its largest negative value at the 9th ring (−0.100 ± 0.0117). The effect of ABH was consistent among genetic clusters for every trait apart from DBH, where population structure was determinant. Excluding the hybrids CSE-ALP, populations from the most northern and southern latitudes

(CSE and ALP) were more influenced by ABH than the other populations (RBA, NPL, and CEU). This trend was not correlated with the latitudinal gradient of DBH, where southern populations have a larger DBH with a higher standard deviation (Table S3).

Ontogenetic shift of population structure and Q_{ST} shows that selection acts primarily upon macroscopic traits

Unlike the Principal Component Analysis (PCA) on raw phenotypes, after correcting for site and block effects with model (1), PCA on the estimated family effects showed a clear population structure (Fig. 4A): genetic clusters were disposed along PC1 (58.9% of variance explained) in decreasing latitudinal order, except for CEU and ALP being reversed. PC1 was mostly driven by DBH, RW, TRW and WD, while PC2 (17.0% of variance explained) was mostly driven by TTW and TWT. That the traits are structured by both family and genetic cluster, is also seen in the fact that intra-family (or intra-population) variance was significantly increased when the family (or population) structure was shuffled (Supplementary Information, methods B).

At the 13th ring, population structure was stronger for macroscopic, growth-related traits than for traits related to tracheid dimensions, density included (Fig. 4B), as the significance of the genetic cluster effect in model (2) was large for DBH and RW ($\chi^2 > 131.26$, df = 5, $p < 10^{-5}$), intermediate for WD and TWT ($\chi^2 > 79.51$, df = 5, $p < 10^{-5}$), and low for TRW and TTW ($\chi^2 < 19.39$, df = 5, $p < 10^{-2}$). The significance of TWT is most likely due to its high correlation with the significant WD ($\rho = 0.88$). Population structure was also stronger at later rings, as the analysis of variance showed an increasing significance over time for every trait (Student's $t > 4.36$, $p < 0.00181$), apart from TRW ($t = -0.706$, $p < 0.498$) and TTW ($t = -2.63$, $p = 0.0274$). This increase most affected growth-related macroscopic traits, namely DBH and RW (Fig. 4B). The strong relation between population structure and ontogenetic shifts can be caused either (i) by bottlenecks (that led to the population structure in Norway spruce) only affecting genes that are expressed at later stages of life by pure luck, or, more likely, (ii) by population specific adaptations expressed at early stages that accentuated population differentiation over time (here, mostly on growth-related traits).

The ontogenetic shift of population structure is most likely the signature of population specific adaptations at early stage population specific adaptations in growth-related macroscopic traits, as Q_{ST} was significantly higher than F_{ST} (Fig. 5) only for DBH ($p = 0.0115$), RW ($p = 0.0086$), and slightly for TTW ($p = 0.0437$), but surprisingly not for ABH (p

= 0.2240). Overall, phenotypic divergence in growth-related macroscopic traits (DBH and RW) can thus be inferred to be due to divergent selection rather than pure drift. Despite the Q_{ST} of TTW being slightly significative, what is striking is that TRW, which is a component of DBH and RW, is not (p = 0.2680). Although interpreting the difference between Q_{ST} and F_{ST} can be fraught with difficulties, one could note that whatever the distribution of F_{ST}, selection, if any, would primarily act upon growth-related macroscopic traits (Fig. 5). Altogether, divergent selection acting at early stages of life led to the accumulation of a selective advantage over time, putatively competitive, as is supported by our analysis of ontogenetic shift of population structure and the trait-wise Q_{ST} *vs* F_{ST}.

If selection on quantitative traits acts as a shift of allele frequencies of Quantitative Trait Loci (QTL), a genome scan would detect signature of such selection. However, in the GWASs on the 66 traits, population structure was a confounding factor with genetic control for every single trait, as significant SNPs were removed when correcting for population structure and/or for kinship (Fig. 4C, 4D). When correcting for population structure and/or kinship in the GWASs (M*, K, or K*), estimated p-values followed a uniform distribution with a 95% confidence (Fig. 4E, 4F), as the distance D was negative for at least 64 out of 66 traits. Only the 8th ring wood density had some SNPs more significant than expected (D = 0.0662), but none of the SNPs were significant after re-estimating the effect size with the adaptive shrinkage framework (p > 0.201). As a matter of fact, correcting our sample for population structure or kinship flattened, or even overcorrected, the genetic signals on the Manhattan plots, since, when no correction was applied, SNPs were more significant than expected for 41 out of 66 traits. GWASs within the largest genetic cluster CSE were also inconclusive, as the distance D was also always negative (except for the 3rd ring WD), with or without correcting for kinship (Fig. S4).

Discussion

The Swedish breeding program is a mixture of local and recently introduced trees from other European countries. As such, although incomplete, the progeny trials reflect the population structure due to glaciation events and constitute a prominent resource of information for evolutionary biology (Chen et al., 2019; Milesi et al., 2019). The breeding conditions constituted a unique opportunity to study competition with conspecifics, by ruling out recruitment selection and considerably lowering interspecific competition. Furthermore, by correcting for population structure and using common garden experiments, we can rule out neutral and plastic processes so that the observed phenotypic differences can be interpreted as being the outcome of adaptation (Savolainen et al., 2013; de Villemereuil et al., 2020). In our common garden experiments, growth exhibited a high level of population differentiation, as expected (Savolainen et al., 2007; Kremer et al., 2012). The growth rate was generally differentiated among individual trees at early stages, supporting the fact that young ages are the most dynamic phases (Lundqvist et al., 2018). In particular, population structure was stronger for trunk diameter than for wood density or its components at the tracheid level.

Divergent selection primarily acted upon resultant growth-related traits

The phenotypes showed a clear latitudinal component at both the genetic and the phenotypic level, as previously reported in Norway spruce (e.g., Milesi et al., 2019; Li et al., preprint) and in other species (e.g., Sang et al., 2019; Csillery et al., 2020). Since local adaptation matches the environment (Savolainen et al., 2013) and colonization routes follow environmental gradients (Gaggiotti et al., 2009; Li et al, preprint), population structure of Norway spruce is, as a result, strongly confounded with local adaptation. Therefore, when assessing the genetic control underlying adaptation of Norway spruce, not correcting for population structure in GWASs, will lead to a high false positive rate (Barton et al., 2019; Lawson et al., 2019), and correcting for population structure, may remove true association, i.e., lead to a high false negative rate. Correctly assessing the genetic variants underlying phenotypic variation is then not possible when there is such a strong latitudinal component. Increasing the number of samples or the number of SNPs remains inconclusive (Chen et al., 2021). Surprisingly, running a GWAS within one genetic cluster was also inconclusive, suggesting that all the adaptive signals were carried out by the shift in allele frequencies between genetic clusters. A possible workaround suggested by Milesi et al. (2019) is to consider phenotypes that are less latitudinally associated, such as the longitudinally associated bud burst, and correct other phenotypes by the population structure thereby

inferred. Alternatively, we can consider several species as suggested by Alberto et al. (2013).

The other side of the coin is that population structure is a good predictor of selection in Norway spruce, as previously reported (Collignon et al. 2002; Savolainen et al., 2007; Kremer et al. 2010). Supporting this, our results on Q_{ST} *vs* F_{ST} showed a clear sign of divergent selection for some traits, suggesting that demographic expansions of Norway spruce in heterogeneous environments led to bottlenecks but also to divergent selection. This is consistent with the hypothesis that most adaptation is reflected by cluster specific allele frequencies (Kremer et al., 2012). The strongest effect of population structure and Q_{ST} was observed for growth-related traits, and secondly for wood density, suggesting that most of the adaptation is associated with radial or upright growth – and therefore with competition. Divergent selection acting at early stages of life most likely led to the accumulation of a competitive advantage, causing then an observable ontogenetic shift of population structure. The average value of F_{ST} was slightly lower than previously reported (0.0488 in our study, and ~0.116-0.145 in Table 1 of Chen et al., 2019), and the interpretation of Q_{ST} *vs* F_{ST} remains controversial (e.g., Whitlock, 2008; Edelaar et al., 2011). However, overall, correcting the estimates of F_{ST} would not change the conclusion of our study: if there is selection, it would primarily affect growth-related macroscopic traits than wood density or its microscopic components. Consistently, the PCA on family effects (Fig. 4A) showed that the latitudinal component – and so, population structure – was mostly explained by trunk diameter, ring width and wood density. Neutral divergence could not be excluded for early growth rate (ABH) in spite of its clear relation with growth. Either this trait is neutral, which is highly unlikely as early stage selection is known to be strong (e.g., Saleh et al., 2022), or, more likely, selection on ABH is invariant among genetic clusters. In the latter case, selection on early growth rate would be strong regardless of the heterogeneity of the locations, where variability would not come from divergence but from, for instance, trade-offs with other life-history traits (e.g., wood density).

The difference between Q_{ST} and F_{ST} is imputed to the covariance between effect sizes, and the covariance between allelic frequencies (reviewed in Le Corre & Kremer, 2012). These covariances can hardly be detected by a GWAS, which might explain the discrepancy between our analyses of Q_{ST} *vs* F_{ST}, showing a strong signal of selection, and our GWASs, showing no signal at all. Altogether, the resulting pattern is that adaptation is more tightly associated to traits that are resultants rather than to its components, in agreement with

Caballero (2020, p. 253). Indeed, components can have random variations that are invisible to selection – therefore neutral, as long as the components contribute to a resultant that is fit. In other words, components have a higher degree of freedom, and therefore are noisier. Since genetic polymorphism depicted by SNPs are partly linked to selection, genomic selection on resultant – such as trunk diameter – should be much more efficient than on components – such as tracheid traits. Determining the genetic basis of such adaptations would need further analyses with a larger sample size of phenotyped individuals, increasing then the statistical power of genomic evaluation and enabling to accounting for covariance at the genetic level in the analyses.

Competition as a core dynamic of demographic expansion

Phenotypes expressed at later stages of tree's life are controlled by genetics and environment, but the continued development of a tree is also influenced by advantages acquired in its early stages. ABH, being a measure of the lag between the tree age and the cambial age at breast height, is a proxy of the early growth rate, and studying its effect amounts to an investigation of the consequence of acquiring early advantages. Every phenotype considered here is associated to fitness in one way or another, but its low heritability, high genetic variance and high environmental variance suggests that ABH is more closely associated to fitness than the investigated tracheid traits (Houle, 1992; Caballero, 2020, p.235). Growth is, however, not to be confounded with fitness. Indeed, individuals from southern populations do not grow faster, but during a longer period. Therefore, transplanting them in Northern Sweden would increase the probability of frost damage and lower their fitness, creating thus a negative correlation between growth and fitness.

Fast growing trees, which reach breast height earlier, have an upper hand in competition by acquiring an asymmetric advantage for light and space resources. This was reflected in our experiment in wider annual rings between cambial ages 5 and 9. While this is the general pattern, individual trees may overtake others and rise in social status within the stand. The cambial age at which such competition starts is most likely driven by the tree-to-tree distance. Increasing the distance will likely increase growth on average, but delay the competition resulting in social differentiation, in accordance with the observed association between population density and competition (reviewed in Biging & Dobertin, 1995; Wisz et al., 2013; or in Tomiolo & Ward, 2018a). In other words, with a sufficiently low population density, our results suggest that slow growers can become larger at later stages, and the

expected shift in woody species from facilitation to competition across ontogenetic stages (Callaway, 1995; Miriti, 2006; Tomiolo & Ward, 2018b) might be ascribed to population density.

Early growth rate was associated to the different genetic clusters, up until later stages of life where the ability to benefit from early advantages (larger negative effect of ABH on DBH) is specific to each population: following the past demography inferred by Chen et al. (2019) and excluding CSE-ALP, in western populations (CSE, CEU and ALP) this ability was the highest in the cluster ALP, and in eastern populations (NPL and RBA) it was the highest in the cluster RBA. The trend seems uncorrelated with both latitude and longitude, but is consistent with the distance to former refugia. Refugia might however hardly be associated with core populations, as genetic load was not especially higher in these populations: π_N/π_S was high regardless of the population (Chen et al., 2019). Trees have the specificity of combining long-generation time and long dispersal (Kremer et al., 2012) and Norway spruce is probably not an exception to the core-front trade-off of competitive *vs* dispersal abilities (Burton et al., 2010), and not insensitive to successive bottlenecks during the expansion despite their large effective population sizes (Excoffier et al., 2009). The global latitudinal pattern affects western and eastern populations differently, but assessing its reason needs further investigations on a smaller geographical scale.

Conclusion

As expected, the pattern of phenotype variation was associated with population structure. The fact that the phenotypes were latitudinally ordered suggests that the origin of population was strongly confounded with adaptation. Teasing apart the demographic history and the adaptation history is challenging, more so that it has been demonstrated that population history had a strong impact on phenotypic divergence in Norway spruce (Lagercrantz & Ryman, 1990; Milesi et al., 2019). However, divergence of phenotypic traits is not necessarily associated with recent population history. Some of the adaptations displayed by Norway spruce were associated to ancestral environments, and some to current environments. In accordance with previous studies (Savolainen et al., 2013; Milesi et al., 2019; Martinez-Sancho et al., 2021), our results support the hypothesis that the current distribution of Norway spruce rather reflects adaptations to ancestral environments than to current ones, as signature of selection was associated with population structure older than the Last Glaciation Maximum. We posit that the quantitative association between phenotypes, latitudes, and population structure would not be observed if there were no local

adaptation to ancestral environments. The last post-glacial expansion of Norway spruce was thus mainly shaped by adaptations *formerly* acquired – not *newly* acquired. In other words, the current distribution of Norway spruce phenotypes is explained by the relation of the current environment to the ancestral environments. Moreover, divergent selection mainly acted upon resultant macroscopic growth-related traits than upon its microscopic components, or wood density. Following the growth-survival trade-off, adaptations in wood density are more survival-related, and those in trunk diameter are more growth-related (reviewed in Falster & Westoby, 2005). Assuming that growth is more driven by competition for light and space than survival is, the current distribution was then strongly influenced by past adaptation to competition.

Author contribution

SL, RGG, and BK designed the study; TG, LO and SL performed experiments or field work and contributed data; PM, ML and RGG contributed genomic data; MT and PM analyzed the data; MT, PM, ML, SL, RGG drafted the manuscript. All authors read and approved the final version of the manuscript.

Data Availability

The data that support the findings of this study are openly available in [repository name e.g "figshare"] at http://doi.org/[doi], reference number [reference number].

Acknowledgements

The authors acknowledge the Swedish research program Bio4Energy and Skogforsk for access to phenotypic data, and the Swedish Foundation for Strategic Research (SSF), grant number RBP14-0040 for exome capture data. This study was funded by the following sources: Uppsala University, SLU Umeå, and the European Union's Horizon 2020 B4Est for basic functioning and postdoc grant for MT. The authors would also like to thank Sophie Karrenberg and Zhi-Qiang Chen for their useful feedback. The computations and data handling were enabled by resources provided by the Swedish National Infrastructure for Computing (SNIC) at UppMax partially funded by the Swedish Research Council through grant agreement no. 2018-05973.

References

Alberto, F. J., Aitken, S. N., Alía, R., et al. (2013). Potential for evolutionary responses to climate change–evidence from tree populations. *Global change biology*, 19(6):1645–1661.

Augspurger, C. K., & Kelly, C. K. (1984). Pathogen mortality of tropical tree seedlings: experimental studies of the effects of dispersal distance, seedling density, and light conditions. *Oecologica*, 61:211–217.

Barton, N., Hermisson, J., & Nordborg, M. (2019). Population genetics: why structure matters. *eLife*, 8:e45380

Bates, D., Mächler, M., Bolker, B., & Walker, S. (2015). Fitting linear mixed-effects models using lme4. *Journal of Statistical Software*, 67(1):1–48.

Bennett, K. D. (1997). *Evolution and ecology: the pace of life*. Cambridge University Press, Cambridge, UK.

Bernhardsson, C., Vidalis, A., Wang, X., et al. (2019). An ultra-dense haploid genetic map for evaluating the highly fragmented genome assembly of Norway spruce (*Picea abies*). *G3 Genes|Genomes|Genetics*, 9:1623–1632.

Biging, G. S., & Dobbertin, M. (1995). Evaluation of competition indices in individual tree growth models. *Forest science*, 41(2):360–377.

Binney, H.A., Willis, K.J., Edwards, et al. (2009). The distribution of late-Quaternary woody taxa in northern Eurasia: evidence from a new macrofossil database. *Quaternary Science Reviews,* 28:2445–2464.

Burton, O. J., Phillips, B. L., & Travis, J. M. (2010). Trade-offs and the evolution of life-histories during range expansion. *Ecology Letters*, 13:1210–1220.

Caballero, A. (2020). Quantitative Genetics (p. 235). Cambridge University Press.

Callaway, R. M. (1995). Positive interactions among plants. *The Botanical Review*, 61(4):306–349.

Case, T. J., Holt, R. D., McPeek, M. A., & Keitt, T. H. (2005). The community context of species' borders: ecological and evolutionary perspectives. *Oikos*, 108:28–46.

Chang, C. C., Chow, C. C., Tellier, L. C. A. M., Vattikuti, S., Purcell, S. M., & Lee, J. J. (2015). Second-generation PLINK: rising to the challenge of larger and richer datasets. *GigaScience*, 4(1).

Chave, J., Coomes, D., Jansen, S., Lewis, S. L., Swenson, N. G., & Zanne, A. E. (2009). Towards a worldwide wood economics spectrum. *Ecology Letters*, 12(4):351–366.

Chen, J., Källman, T., Ma, X., et al. (2012). Disentangling the roles of history and local selection in shaping clinal variation of allele frequencies and gene expression in Norway spruce (*Picea abie*s). *Genetics*, 191(3):865–881.

Chen, Z. Q., García-Gil, M. R., Karlsson, B., Lundqvist, S.-O., Olsson, L., & Wu, H. X. (2014). Inheritance of growth and solid wood quality traits in a large Norway spruce population tested at two locations in southern Sweden. *Tree Genetics & Genomes*, 10(5):1291–1303.

Chen, Z. Q., Karlsson, B., Mörling, T., et al. (2016). Genetic analysis of fiber dimensions and their correlation with stem diameter and solid-wood properties in Norway spruce. *Tree Genetics & Genomes*, 12(6):1–12.

Chen, J., Li, L., Milesi, P., et al. (2019). Genomic data provide new insights on the demographic history and the extent of recent material transfers in Norway spruce. *Evolutionary Applications*, 12:1539–1551.

Chen, Z.-Q., Zan, Y., Milesi, P., et al. (2021). Leveraging breeding programs and genomic data in Norway spruce (*Picea abies* L. Karst) for GWAS analysis. *Genome Biology*, 22:179.

Collignon, A. M., Sype, H. V. D., & Favre, J. M. (2002). Geographical variation in random amplified polymorphic DNA and quantitative traits in Norway spruce. *Canadian Journal of Forest Research*, 32(2):266–282.

Coomes, D. A., Heathcote, S., Godfrey, E. R., Shepherd, J. J., & Sack, L. (2008). Scaling of xylem vessels and veins within the leaves of oak species. *Biology Letters*, 4(3):302–306.

Crawley, M. J. (2007). Statistical modelling. In *The R book* (pp. 323–386). Chichester, UK.

Csilléry, K., Ovaskainen, O., Sperisen, C., Buchmann, N., Widmer, A., & Gugerli, F. (2020). Adaptation to local climate in multi-trait space: evidence from silver fir (Abies alba Mill.) populations across a heterogeneous environment. *Heredity*, 124(1):77–92.

Danecek, P., Auton, A., Abecasis, G., Albers, C. A., Banks, E., DePristo, et al. (2011). The variant call format and VCFtools. *Bioinformatics*, 27(15):2156–2158.

De Villemereuil, P., Gaggiotti, O. E., & Gouder, J. (2020). Common garden experiments to study local adaptation need to account for population structure. *Journal of Ecology*, 00:1–5.

Edelaar, P. I. M., & Björklund, M. (2011). If FST does not measure neutral genetic differentiation, then comparing it with QST is misleading. Or is it?. *Molecular Ecology*, 20(9):1805–1812.

Enquist, B. J., West, G. B., Charnov, E. L., & Brown, J. H. (1999). Allometric scaling of production and life-history variation in vascular plants. *Nature*, 401:907–911.

Evans, R. (1994) Rapid measurement of the transverse dimensions of tracheids in radial wood sections from Pinus Radiata. *Holz-forschung*, 48:168–172

Evans, R. (2006) Wood stiffness by X-ray diffractometry (pp 138–146). In: Stokke DD, Groom HL (eds) Characterization of the cellulosic cell wall. Wiley, Hoboken.

Excoffier, L., Foll, M., & Petit, R. J. (2009). Genetic consequences of range expansions. *Annual Review of Ecology, Evolution, and Systematics*, 40:481–501.

Falconer, D.S. (1989). *Introduction to quantitative genetics* (3rd edition, p. 116). Pearson Education India.

Falster, D. S. & Westoby, M. (2003). Plant height and evolutionary games. *Trends in Ecology & Evolution*, 18(7):337–343.

Falster, D. S. & Westoby, M. (2005). Alternative height strategies among 45 dicot rain forest species from tropical Queensland, Australia. *Journal of Ecology*, 93(3):521–535.

Givnish, T. J. (1982). On the adaptive significance of leaf height in forest herbs. *The American Naturalist*, 120(3):353–381.

Houle, D. (1992). Comparing evolvability and variability of quantitative traits. *Genetics*, 130(1):195–204.

Iwasa, Y., Cohen, D., and Léon, J. A. (1985). Tree height and crown shape, as results of competitive games. *Journal of Theoretical Biology*, 112(2):279–297

Kitajima, K. (1994). Relative importance of photosynthetic traits and allocation patterns as correlates of seedling shade tolerance of 13 tropical trees. *Oecologica*, 98:419–428.

Kremer, A., Le Corre, V., Petit, R. J., & Ducousso, A. (2010). Historical and contemporary dynamics of adaptive differentiation in European oaks. *Molecular approaches in natural resource conservation*, 101–122.

Kremer, A., Ronce, O., Robledo-Arnuncio, et al. (2012). Long-distance gene flow and adaptation of forest trees to rapid climate change. *Ecology letters*, 15(4):378–392.

Lagercrantz, U., & Ryman, N. (1990). Genetic structure of Norway spruce (Picea abies): concordance of morphological and allozymic variation. *Evolution*, 44(1):38–53.

Lawson, D. J., Davies, N. M., Haworth, et al. (2019). Is population structure in the genetic biobank era irrelevant, a challenge, or an opportunity? *Human Genetics*, 139:23–41.

Le Corre, V., & Kremer, A. (2012). The genetic differentiation at quantitative trait loci under local adaptation. *Molecular ecology*, 21(7):1548–1566.

Li, H., Handsaker, B., Wysoker, A., Fennell, T., et al. (2009). The sequence alignment/map format and SAMtools. *Bioinformatics*, 25(16):2078–2079.

Li, H. & Durbin, R. (2010). Fast and accurate long-read alignment with Burrows–Wheeler transform. *Bioinformatics*, 26(5):589–595

Li, L., Milesi, P., Tiret, M., et al. Teasing apart the joint effect of demography and natural selection in the birth of a contact zone. *bioRxiv*, 2022.01.11.475794.

Lundqvist, S.-O., Seifert, S., Grahn, T., et al. (2018). Age and weather effects on between and within ring variations of number, width and coarseness of tracheids and radial growth of young Norway spruce. *European Journal of Forest Research*, 137:719–743.

Martínez-Sancho, E., Rellstab, C., Guillaume, F., et al. (2021). Post-glacial re-colonization and natural selection have shaped growth responses of silver fir across Europe. *Science of the Total Environment*, 779:146393.

McKenna, A., Hanna, M., Banks, E., et al. (2010). The genome analysis toolkit: a MapReduce framework for analyzing next-generation DNA sequencing data. *Genome Research*, 20(9):1297–1303.

Milesi, P., Berlin, M., Chen, J., et al. (2019). Assessing the potential for assisted gene flow using past introduction of Norway spruce in southern Sweden: local adaptation and genetic basis of quantitative traits in trees. *Evolutionary Applications*, 12(10):1946–1959.

Miriti, M. N. (2006). Ontogenetic shift from facilitation to competition in a desert shrub. *Journal of Ecology*, 94(5):973–979.

Montwé, D., Isaac-Renton, M., Hamann, A., & Spiecker, H. (2016). Drought tolerance and growth in populations of a wide-ranging tree species indicate climate change risks for the boreal north. *Global Change Biology*, 22(2):806–815.

Niklas, K. J. (1993). Influence of tissue density-specific mechanical properties on the scaling of plant height. *Annals of Botany*, 72(2):173–179.

Nota, K., Klaminder, J., Milesi, P., Bindler, R., Nobile, A., van Steijn, T., et al. (2022). Norway spruce postglacial recolonization of Fennoscandia. *Nature Communications*, 13(1):1–9.

Nystedt, B., Street, N. R., Wetterbom, A., et al. (2013). The norway spruce genome sequence and conifer genome evolution. *Nature*, 497:579–584.

Orsucci, M., Milesi, P., Hansen, J., Girodolle, J., Glémin, S., & Lascoux, M. (2020). Shift in ecological strategy helps marginal populations of shepherd's purse (Capsella bursa-pastoris) to overcome a high genetic load. *Proceedings of the Royal Society B: Biological Sciences*, 287(1927):20200463.

Palmé, A. E., Su, Q., Rautenberg, A., Manni, F., & Lascoux, M. (2003). Postglacial recolonization and cpdna variation of silver birch, *Betula pendula*. *Molecular Ecology*, 12:201–212.

Petit, R. J., Brewer, S., Bordács, S., et al. (2002). Identification of refugia and post-glacial colonisation routes of European white oaks based on chloroplast DNA and fossil pollen evidence. *Forest ecology and management*, 156(1-3):49–74.

Petit, R. J., Aguinagalde, I., De Beaulieu, J.-L., et al. (2003). Glacial refugia: hotspots but not melting pots of genetic diversity. *Science*, 300(5625):1563–1565.

Poorter, L., Bongers, L., & Bongers, F. (2006). Architecture of 54 moist-forest tree species: traits, trade-offs, and functional groups. *Ecology*, 87(5):1289–1301.

Poorter, L. (2008). The relationships of wood-, gas-and water fractions of tree stems to performance and life history variation in tropical trees. *Annals of botany*, 102(3):367–375.

Poorter, L., McDonald, I., Alarcón, A., et al. (2010). The importance of wood traits and hydraulic conductance for the performance and life history strategies of 42 rainforest tree species. *New Phytologist*, 185(2):481–492.

Preston, K. A., Cornwell, W. K., & DeNoyer, J. L. (2006). Wood density and vessel traits as distinct correlates of ecological strategy in 51 California coast range angiosperms. *New Phytologist*, 170(4):807–818.

Pretzsch, H., Biber, P., Schütze, G., Kemmerer, J., & Uhl, E. (2018). Wood density reduced while wood volume growth accelerated in Central European forests since 1870. *Forest Ecology and Management*, 429:589–616.

R Core Team (2021). R: A language and environment for statistical computing. R Foundation for Statistical Computing, Vienna, Austria. URL: https://www.R-project.org/.

Riis, T., Lambertini, C., Olesen, B., Clayton, J. S., Brix, H., & Sorrell, B. K. (2010). Invasion strategies in clonal aquatic plants: are phenotypic differences caused by phenotypic plasticity or local adaptation? *Annals of Botany*, 106(5):813–822

Rossi, S., Cairo, E., Krause, C., & Deslauriers, A. (2015). Growth and basic wood properties of black spruce along an alti-latitudinal gradient in Quebec, Canada. *Annals of Forest Science*, 72:77–87.

Saleh, D., Chen, J., Leplé, J. C., Leroy, T., Truffaut, L., Dencausse, et al. (2022). Genome-wide evolutionary response of European oaks during the Anthropocene. *Evolution letters*, 6(1):4–20.

Sang, Z., Sebastian-Azcona, J., Hamann, A., Menzel, A., & Hacke, U. (2019). Adaptive limitations of white spruce populations to drought imply vulnerability to climate change in its western range. *Evolutionary Applications*, 12(9):1850–1860.

Savolainen, O., Pyhäjärvi, T., & Knürr, T. (2007). Gene flow and local adaptation in trees. *Annu. Rev. Ecol. Evol. Syst.*, 38:595–619.

Savolainen, O., Lascoux, M., & Merilä, J. (2013). Ecological genomics of local adaptation. Nature Reviews Genetics, 14:807–820.

Spitze, K. (1993). Population structure in Daphnia obtusa: quantitative genetic and allozymic variation. *Genetics*, 135(2): 367–374.

Stephens, M. (2017). False discovery rates: a new deal. *Biostatistics*, 18(2):275–294.

Suarez, A. V., & Tsutsui, N.D. (2008). The evolutionary consequences of biological invasions. *Molecular ecology,* 17(1):351–360.

Tiret, M., & Milesi, P. Statistical Peak Detection for GWAS. Zenodo. https://doi.org/10.5281/zenodo.5079556. Deposited 7 July 2021.

Tomiolo, S., & Ward, D. (2018a). Species migrations and range shifts: A synthesis of causes and consequences. *Perspectives in plant ecology, evolution and systematics*, 33:62–77.

Tomiolo, S., & Ward, D. (2018b). Soil properties and climate mediate the effects of biotic interactions on the performance of a woody range expander. *Ecosphere*, 9(4):e02186.

Tsuda, Y., Chen, J., Stocks, M., et al. (2016). The extent and meaning of hybridization and introgression between Siberian spruce (Picea obovata) and Norway spruce (*Picea abies*): cryptic refugia as stepping stones to the west? *Molecular Ecology*, 25(12):2773–2789.

Van der Auwera, G. A., Carneiro, M. O., Hartl, C., et al. (2013). From FastQ data to high-confidence variant calls: the genome analysis toolkit best practices pipeline. *Current Protocols in Bioinformatics*, 43:11.10.1–11.10.33.

Van Gelder, H. A., Poorter, L., & Sterck, F. J. (2006). Wood mechanics, allometry, and life-history variation in a tropical rain forest tree community. *New Phytologist*, 171(2):367–378.

Van Valen, L. (1973). A new evolutionary law. *Evol theory*, *1*: 1–30.

VanWallendael, A., Hamann, E., & Franks, S. J. (2018). Evidence for plasticity, but not local adaptation, in invasive Japanese knotweed (Reynoutria japonica) in North America. *Evolutionary Ecology*, 32:395–410.

Vendramin, G. G., Anzidei, M., Madaghiele, A., Sperisen, C., & Bucci, G. (2000). Chloroplast microsatellite analysis reveals the presence of population subdivision in Norway spruce (*Picea abies* K.). *Genome*, 43(1): 68–78.

Vidalis, A., Scofield, D. G., Neves, L. G., Bernhardsson, C., García-Gil, M. R., & Ingvarsson, P. K. (2018). Design and evaluation of a large sequence-capture probe set and associated SNPs for diploid and haploid samples of Norway spruce (*Picea abies*). *BioRxiv*, 291716.

Von Gadow, K., Álvarez González, J. G., Zhang, C., Pukkala, T., & Zhao, X. (2021). The Shape and Growth of Forest Trees. In *Sustaining Forest Ecosystems* (pp. 159-219). Springer, Cham.

Whitlock, M. C. (2008). Evolutionary inference from QST. *Molecular ecology*, 17(8):1885–1896.

Wisz, M.S., Pottier, J., Kissling, W.D., et al. (2013), The role of biotic interactions in shaping distributions and realised assemblages of species: implications for species distribution modelling. *Biological Reviews*, 88:15–30.

Yang, J., Lee, S. H., Goddard, M. E., & Visscher, P. M. (2011). GCTA: a tool for genome-wide complex trait analysis. *The American Journal of Human Genetics*, 88(1):76–82.

Figure legends and Tables

Figure 1. Overall description of phenotypes and genotypes of the sample of Norway spruce. (A) Principal Component Analysis of the genotypes of the half-sib families. Families are colored according to their genetic clusters (ordered by decreasing latitude in the legend): Central and South Sweden (CSE, dark red), Russia-Baltics (RBA, light green), Northern Poland (NPL, green), Central Europe (CEU, light blue), Alps (ALP, blue), and hybrids between CSE and ALP (CSE-ALP, pink). PC1 and PC2 explained 3.42% and 0.45% of the variance, respectively. **(B)** Admixture plot of the half-sib families, with K = 3. Individuals are grouped by population, and sorted according to their coancestry coefficient. **(C)** Principal Component Analysis of the phenotypes: Diameter at Breast Height (DBH), Ring Width (RW), Wood Density (WD), Tracheid Radial Width (TRW), Tracheid Tangential Width (TTW), and Tracheid Wall Thickness (TWT). Left panel only shows variable axes and 60% confidence ellipses. On the right panel, each data (dot) is colored according to its cambial age (3rd year in light blue up until 13th year in dark blue). PC1 and PC2 explained 41.2% and 38.3% of the variance, respectively.

Figure 2. Effect of population structure on the phenotypes of Norway spruce. Boxplots of different phenotypic traits as a function of the genetic clusters: Central and South Sweden (CSE), Russia-Baltics (RBA), Northern Poland (NPL), Central Europe (CEU), Alps (ALP), and hybrids between CSE and ALP (CSE-ALP). The red dots indicate the mean value. **(A)** Age at Breast Height (ABH). **(B)** 13th ring Diameter at Breast Height (DBH). **(C)** 13th Ring Width (RW). **(D)** 13th ring Wood Density (WD). **(E)** 13th ring Tracheid Radial Width (TRW). **(F)** 13th ring Tracheid Tangential Width (TTW). **(G)** 13th ring Tracheid Wall Thickness (TWT). **(H)** Barplots of the heritability of the traits displayed in panel (A) - (F).

Figure 3. Effect of Age at Breast Height (ABH) on Norway spruce. (A) Boxplots of predicted ABH according to model (1bis) as a function of site (Höreda in dark gray, Erikstorp in light gray) and of genetic cluster: Central and South Sweden (CSE), Russia-Baltics (RBA), Northern Poland (NPL), Central Europe (CEU), Alps (ALP), and hybrids between CSE and ALP (CSE-ALP). **(B)** ANOVA of ABH in model (2) as a function of cambial age (from 3 to 13), and of traits: Diameter at Breast Height (DBH, red), Ring Width (RW, brown), Wood Density (WD, green), Tracheid Radial Width (TRW, turquoise), Tracheid Tangential Width (TTW, blue), and Tracheid Wall Thickness (TWT, pink). **(C)** Estimated effect of ABH in

model (2) (addition of c_l and $(c \times g)_l$ with the notation of model (2)) as a function of cambial age (from 3 to 13), and of traits (idem as panel B), in the trial of Höreda.

Figure 4. Genetic control of wood properties in Norway spruce. (A) Principal Component Analysis of the residuals of the phenotypes according to model (2): Diameter at Breast Height (DBH), Ring Width (RW), Wood Density (WD), Tracheid Radial Width (TRW), Tracheid Tangential Width (TTW), and Tracheid Wall Thickness (TWT). Left panel only shows variable axes and 10% confidence ellipses (zoomed x2.5), where clusters were ordered in decreasing latitude from right to left. On the right panel, each data (dot) is colored according to its genetic cluster (ordered by decreasing latitude in the legend): Central and South Sweden (CSE, dark red), Russia-Baltics (RBA, light green), Northern Poland (NPL, green), Central Europe (CEU, light blue), Alps (ALP, blue), and hybrids between CSE and ALP (CSE-ALP, pink). PC1 and PC2 explained 57.5% and 18.2% of the variance, respectively. **(B)** ANOVA of genetic clusters in model (2) as a function of cambial age (from 3 to 13), and of traits: DBH (plain circle), RW (plain triangle), WD (plain square), TRW (circle), TTW (triangle), and TWT (square). **(C)** Manhattan plot of the GWAS in model (M) of DBH at the 5th ring. The dotted horizontal line is the Bonferroni significance level for n = 118,145. The dashed vertical lines are the location of the peaks of significant SNPs. **(D)** Manhattan plot of the GWAS in model (M*) of DBH at the 5th ring. Legends are identical to panel C. **(E)** Q-Q plot of observed *versus* expected *p*-values (in log scale) on the 5th ring DBH, without any correction (M, in squares), with population structure correction (M*, in plain squares), with kinship correction (K, in circles), and with population structure and kinship corrections (K*, in plain circles). The solid line is a 1-slope line, and the dashed lines are the upper and lower bound of the 95% confidence interval. **(F)** Distance *D* on GWAS (K*) as a function of cambial age and of traits (idem than panel B). The dotted horizontal lines indicate the width of the 95% confidence interval.

Figure 5. Distribution of pairwise F_{ST} across the genome, averaged among pairs of populations. The vertical solid black line is the average F_{ST} over the genome (0.0488), and vertical dotted lines are the Q_{ST} estimated for different traits (averaged across rings): Diameter at Breast Height (DBH, red, Q_{ST} = 0.281), Ring Width (RW, green, Q_{ST} = 0.302), Wood Density (WD, brown, Q_{ST} = 0.121), Tracheid Radial Width (TRW, turquoise, Q_{ST} = 0.0579), Tracheid Tangential Width (TTW, blue, Q_{ST} = 0.177), Tracheid Wall Thickness (TWT, purple, Q_{ST} = 0.112), and Age at Breast Height (ABH, pink, Q_{ST} = 0.066).

	ABH (year)	**DBH (mm)**	**RW (mm)**	**WD ($kg.m^{-3}$)**	**TRW (µm)**	**TTW (µm)**	**TWT (µm)**
σ_F^2	1.90×10^{-3}	3.03×10^{-2}	5.13×10^{-3}	2.77×10^{-3}	5.99×10^{-4}	4.73×10^{-4}	2.47×10^{-3}
$\sigma_B^2 + \sigma^2$	3.29×10^{-2}	2.15×10^{-1}	5.63×10^{-2}	1.95×10^{-2}	6.04×10^{-3}	4.91×10^{-3}	1.88×10^{-2}
h^2 **(%)**	20.87	49.32	33.47	49.80	36.11	35.20	46.52

Table 1. Genetic variance (σ_F^2), environmental variance ($\sigma_B^2 + \sigma^2$), and heritability (h^2) were estimated with model (1). Traits: Calendar age at Breast Height (ABH), Diameter at Breast Height (DBH), Ring Width (RW), Wood Density (WD), Tracheid Radial Width (TRW), Tracheid Tangential Width (TTW), and Tracheid Wall Thickness (TWT).

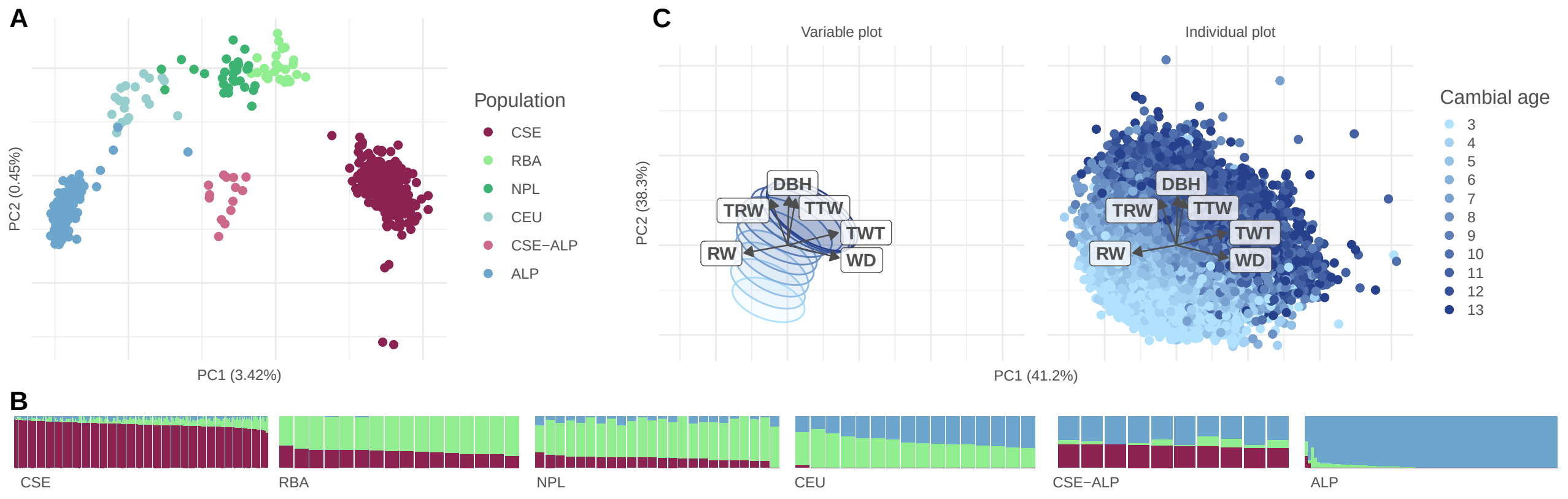
A
PC2 (0.45%)
PC1 (3.42%)
Population
CSE
RBA
NPL
CEU
CSE−ALP
ALP
C
Variable plot
Individual plot
PC2 (38.3%)
PC1 (41.2%)
DBH
TRW
TTW
TWT
RW
WD
Cambial age
3
4
5
6
7
8
9
10
11
12
13
B
CSE
RBA
NPL
CEU
CSE−ALP
ALP

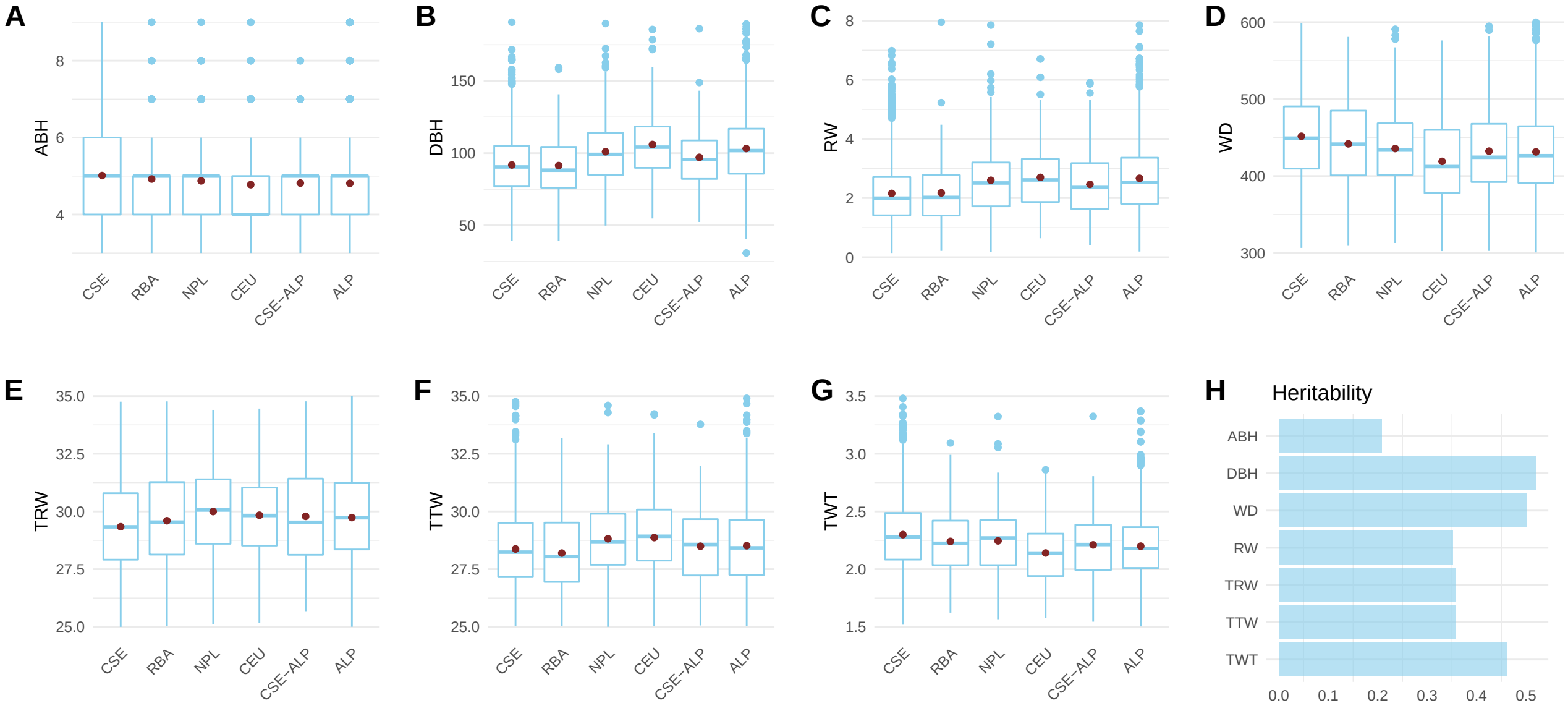
A
ABH
8
6
4
CSE
RBA
NPL
CEU
CSE−ALP
ALP
B
DBH
150
100
50
C
RW
8
6
4
2
0
D
WD
600
500
400
300
E
TRW
35.0
32.5
30.0
27.5
25.0
F
TTW
G
TWT
3.5
3.0
2.5
2.0
1.5
H
Heritability
ABH
DBH
WD
RW
TRW
TTW
TWT
0.0
0.1
0.2
0.3
0.4
0.5

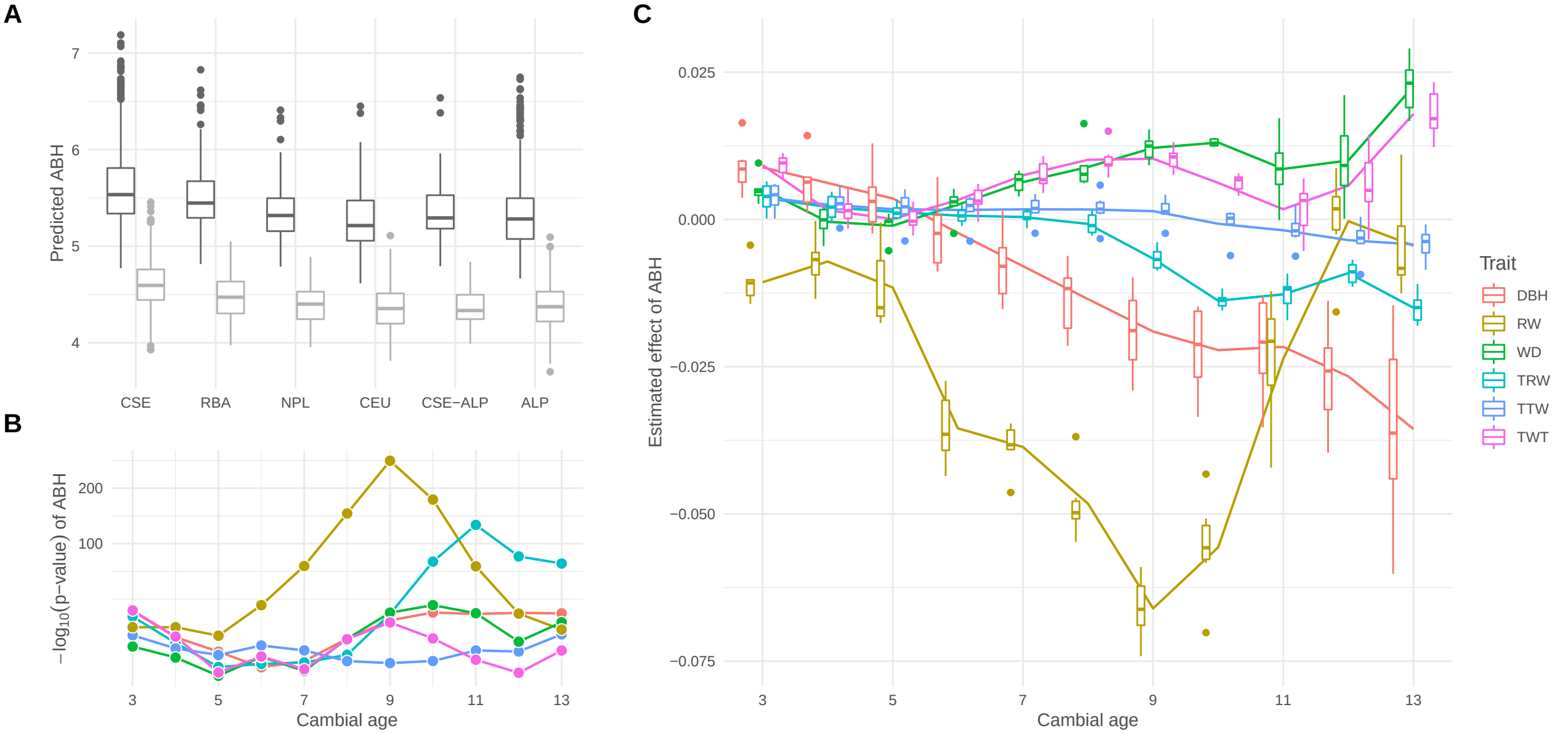
A
Predicted ABH
7
6
5
4
CSE
RBA
NPL
CEU
CSE−ALP
ALP
B
−log10(p−value) of ABH
200
100
3
5
7
9
11
13
Cambial age
C
Estimated effect of ABH
0.025
0.000
−0.025
−0.050
−0.075
3
5
7
9
11
13
Cambial age
Trait
DBH
RW
WD
TRW
TTW
TWT

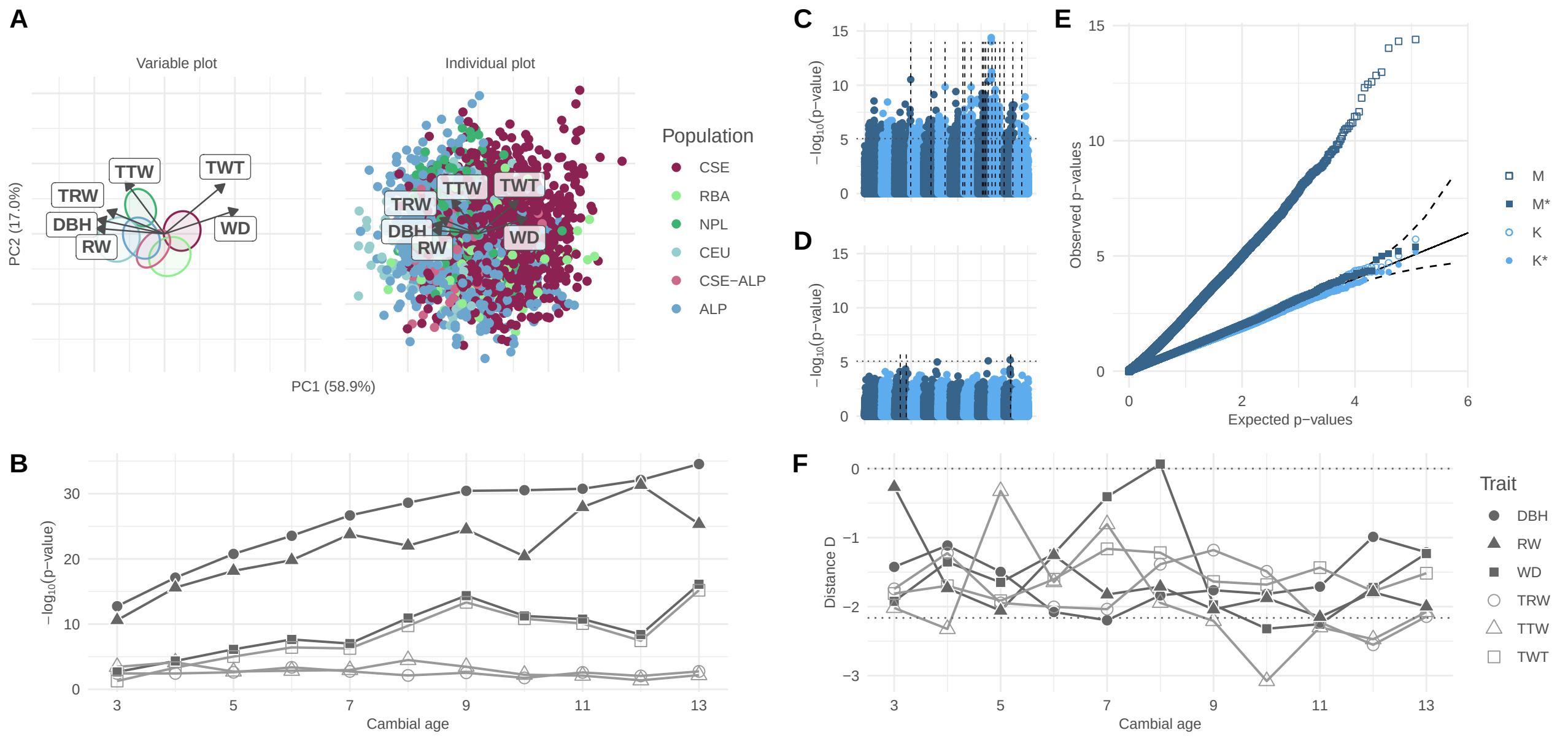
A
Variable plot
Individual plot
TTW
TWT
TRW
DBH
RW
WD
PC2 (17.0%)
PC1 (58.9%)
Population
CSE
RBA
NPL
CEU
CSE−ALP
ALP
C
D
−log10(p−value)
E
Observed p−values
Expected p−values
M
M*
K
K*
B
−log10(p−value)
Cambial age
F
Distance D
Cambial age
Trait
DBH
RW
WD
TRW
TTW
TWT

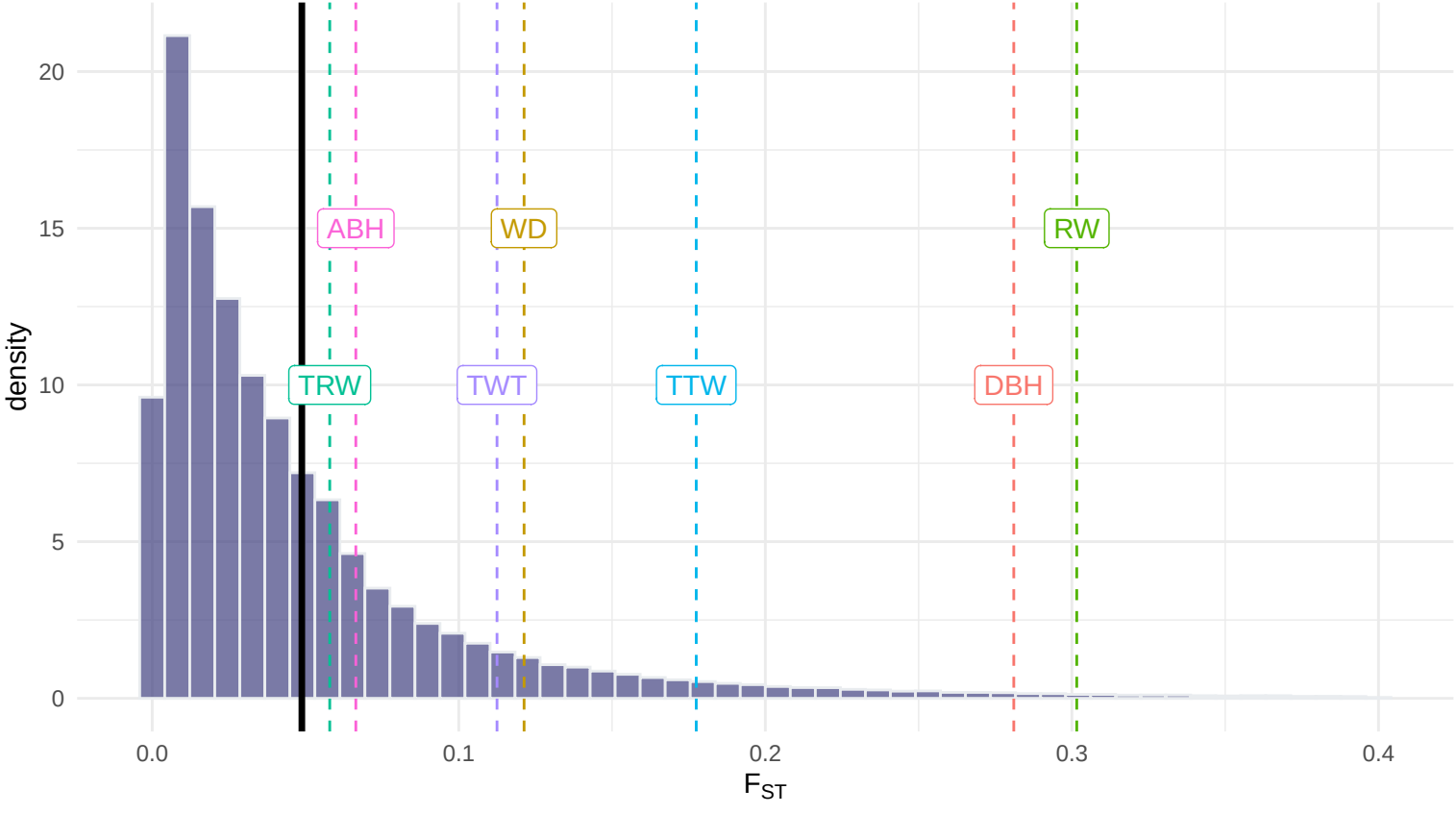
density
20
15
10
5
0
ABH
WD
RW
TRW
TWT
TTW
DBH
0.0
0.1
0.2
0.3
0.4
F_{ST}